Supporting Information

Anchukaitis et al. 10.1073/pnas.0908572107

SI Text

Site Description. The Monteverde Cloud Forest sits astride the continental divide in the Cordillera de Tilaran in northwestern Costa Rica. Above 1,500 m elevation, vegetation is classified montane wet cloud forest (1) and its hydroclimatology is characterized by persistent immersion in the orographic cloud bank formed as the northeasterly trade winds moving across the warm waters of the Caribbean are forced to rise over the cordillera. Higher relative humidity, increased moisture, persistent cloud cover, and reduced temperatures support montane forests rich in endemic organisms and important for local hydrology (2, 3). During boreal summer (May to October), cloud forests receive most of their rainfall as the northward movement of the Intertropical Convergence Zone (ITCZ) brings convective storms to the region. During the dry season (approximately January through April), moisture advection and cloud water deposition are an important component of cloud forest hydrology (4), particularly on the leeward Pacific slope that would otherwise experience the effects of a pronounced dry season.

Stable Isotope Analysis and Interpretation. Following standard convention, oxygen isotope ratios are referenced and reported relative to the international Vienna Standard Mean Ocean Water:

$$\delta^{18}\mathrm{O} = \left(\frac{\frac{^{18}\mathrm{O}}{^{16}\mathrm{O}_{\mathrm{sample}}} - \frac{^{18}\mathrm{O}}{^{16}\mathrm{O}_{\mathrm{ref}}}}{\frac{^{18}\mathrm{O}}{^{16}\mathrm{O}_{\mathrm{ref}}}} \right) \times 1,000. \qquad [\mathrm{S1}]$$

Raw isotope ratio data were corrected based on the value of the solid standard material and measurements of monitoring gas (CO) with a known isotope composition prior to and after every sample. Data quality assurance was assessed based on sample peak voltages, peak shape, background stability, and monitoring gas measurements.

The δ^{18}O time series from MV15 shows an abrupt change in growth rates at approximately 121 mm depth in the core. Accompanying this change is a substantial increase in the amplitude of the final eight annual oxygen isotope cycles. The rapid growth rates which correspond with the inner portion of the core result in an large increase in the number of individual samples per annual cycle. The higher sampling rate could potentially translate into larger amplitude δ^{18}O cycles simply by virtue of more precisely resolving in time short-term changes in water use in the tree. Because this could possibly bias our climatic interpretation of the oxygen isotope time series for this earliest part of our record, for the purpose of climate analysis we statistically downsampled the sampling resolution to 6–10 samples per cycle to simulate that of the outer portion of MV15. Despite this a priori correction, however, the inner part of MV15 still has larger amplitude cycles than much of the outer core, and therefore we interpret this earliest decade cautiously, as these years could still contain a growth rate sampling bias.

Thus far, relatively little information exists about potential "juvenile effects" in oxygen isotope chronologies from trees. Treydte et al. (2006) (5) found that when trees were younger, the δ^{18}O of their xylem cellulose was enriched over that of older trees growing simultaneously. In the case of MV12 and MV15, we do not see any evidence of an enriched mean δ^{18}O in the earliest parts of the cores, and there is no indication that our cores reached pith. It cannot be ruled out that the increased variance in MV15 in the earliest part of the chronology, as discussed above, could be related to a juvenile effect, where younger trees with less extensive root systems use predominantly very shallow ground water; however, our conclusions do not depend on the interpretation of this part of the record. Much interesting work remains to be done to understand how trees might reflect age-related effects in the δ^{18}O of their xylem cellulose.

Heuristic and Mechanistic Model. The origin of annual cycles in the stable oxygen isotope composition of the wood of tropical cloud forest trees is the differential δ^{18}O composition of dry and wet season moisture (6, 7). This hypothesis is not specific to any particular species (6). Annual and interannual oxygen isotope ratios in tropical meteoric waters are primarily controlled by the "amount effect," the inverse relationship between the amount of precipitation and its δ^{18}O value (8, 9). The amount effect is evident in surface waters from Costa Rica and Panama (10) and in seasonal precipitation from Monteverde (11, 12). In montane forests, moisture inputs from clouds are an additional source of water for trees, particularly in the dry season. Cloud water has an enriched isotopic signature similar to tropical dry season rainfall (11, 13, 14, 15, 16). Dry season sources of moisture (the limited amount of rainfall and horizontal precipitation from orographic clouds) provide trees with sufficient water to avoid water stress and potentially the need for a seasonal growth hiatus, but have a distinct isotopic signature.

In order to develop objective, biochemical hypotheses for the mechanistic interpretation of cellulose δ^{18}O in tropical cloud forest trees, we used meteorological (17) and stable isotope data (11, 12) from Monteverde to simulate the sensitivity of δ^{18}O of cellulose in cloud forest trees to climate anomalies. The major obstacle to this exercise is the lack of any relative humidity, wind data, or cloud observations from within the cloud forest itself. Anchukaitis et al. (2008) (7) were able to successfully simulate annual isotope cycles and their interannual variability in trees from *below* the main cloud forest elevations using the temperature and precipitation data from the Campbell weather station (17) and the relative humidity data modeled from a short period of meteorological observations in the premontane forest downslope from the Cloud Forest Reserve (11). For the *Pouteria* trees within the cloud forest itself in the current study, however, we have no reliable record of either the time variability or annual climatology of relative humidity.

We use the Barbour et al. (2004) (18) model of the environmental controls on the stable isotope composition of wood, as modified and adapted by Evans (2007) (19), to simulate theoretical monthly stable oxygen isotope climatology. The model has previously been described in detail and deployed for temporal simulations (19, 7). Briefly, the model simulates cellulose δ^{18}O as a function of temperature, precipitation, and relative humidity data. Many model parameters (18) are only weakly constrained by observations, particularly for tropical species and environments. Uncertainties in these parameters influence the resulting simulation by changing both the mean and standard deviation, and estimates of the δ^{18}O of cellulose have uncertainties as large as ~1‰ if we assume 20% uncorrelated errors in each of 14 variable parameters (7, 19). Nearly all of this uncertainty arises, however, from a dilation or contraction of the overall time series variance, while year-to-year patterns of variability remain the same (7). We estimated leaf temperature as a function of air temperature (20). Atmospheric water vapor δ^{18}O is calculated as a function of estimated condensation temperature (21). Stomatal conductance is calculated as a function of the vapor pressure deficit, which is derived from the monthly air temperature, the

derived leaf temperature, and relative humidity. The $\delta^{18}O$ of water at the site of photosynthesis in the leaves is calculated as a change in the source water $\delta^{18}O$ as a function of the kinetic and equilibrium diffusive fractionation, leaf temperature, water vapor $\delta^{18}O$, and the vapor pressure gradient between the leaf and atmosphere.

We use this model to develop hypotheses for the sign and potential magnitude of the response of $\delta^{18}O$ to climate variability. Daily values for temperatures and precipitation from the Campbell station (17) were combined to form monthly mean and total precipitation climatology for model input. For relatively humidity, we extracted a time series of monthly values from the NCEP Reanalysis II gridded data (22, 23) for the latitude, longitude, and atmospheric pressure level (850 mb) which most closely corresponds to the Monteverde Cloud Forest. Following Anchukaitis et al. (2008) (7), we calculated monthly source water $\delta^{18}O$ values as a function of the observed relationship between rainfall amount and the $\delta^{18}O$ composition of rainfall from Rhodes et al. (2006) (11). We regressed the $\delta^{18}O$ on rainfall amounts for those data with aggregate collection periods of two weeks to two months. We determined that shorter collection periods showed a higher variability that might reflect the time of sampling and the trajectory and history of individual weather systems. Longer sampling periods excessively smoothed monthly differences related to the timing of precipitation seasonality. Source water $\delta^{18}O$ values were calculated based on monthly total precipitation values from the Campbell (17) dataset. Our regression model accounts for 56% of the variance in the observed dataset and is significant at $p < 0.01$ with 14 effective degrees of freedom.

We created three hypotheses to predict the response of annual $\delta^{18}O$ cycles to climate variability. First, we calculated an overall mean $\delta^{18}O$ cycle ("control") by averaging the monthly values from all years with available climate data. We then ran the model with imposed monthly wet season (May-October) precipitation and $\delta^{18}O$ values equal to that of the observed maximum observed rainfall for those months for all years. We also created two mean $\delta^{18}O$ cycles where the dry season relative humidity was replaced by the maximum or minimum observed relative humidity for those months for all years. The mean of the experimental model simulation was set such that the means of the *nonexperimental* season (dry or wet) was the same as that in the simulation created using the unaltered, observed climate data. In this way the expected interannual magnitude of the model-generated anomalies relative to the control could be isolated for each season (corresponding to the maxima and minima of the annual $\delta^{18}O$ cycle).

These process modeling experiments provide biophysical support for the existence of annual $\delta^{18}O$ cycles in cellulose arising from the annual wet and dry seasons that can be used for chronological control (Fig. S1, compare with observed annual isotope cycle in Fig. 2*A*). Model experiments demonstrate that anomalies in this cycle of 1‰ or more can be generated by anomalous wet season rainfall or dry season relative humidity observed over the short instrumental or Reanalysis period. Note also that wet season rainfall anomalies carry over to the following dry season and influence the annual cycle amplitude in this manner. Modeling results provide quantitative support for climatic interpretation of isotope variability to complement statistical analysis.

We emphasize that, despite uncertainties in the parameter set for the model (7, 18, 19), these almost entirely result in changes in the mean or standard deviation of the overall time series, but have almost no effect on relative magnitude of the mean $\delta^{18}O$ annual cycle compared to the amplitude anomalies associated with the sensitivity experiments described above. The annual cycle is dominated by the existence of the amount effect in the annual cycle of precipitation $\delta^{18}O$ (19) and the anomalies by changes in relative humidity and precipitation amount. This has been previously documented in other $\delta^{18}O$ cellulose modeling studies at monthly resolution (7, 19). Model code in MATLAB is available via the NOAA NCDC World Data Center, ftp://ftp.ncdc.noaa.gov/pub/data/paleo/treering/isotope/northamerica/costarica/evans2007/evans2007.txt. The original Microsoft Excel version of the model (18) is available from the University of Utah, http://ecophys.biology.utah.edu/public/Tree_Ring/.

Radiocarbon Dating. Wood and cellulose samples were selected in order to provide high-resolution dates using the ^{14}C signature of atmospheric atomic weapons testing (24). Four samples were wood that we preprocessed using an acid-base-acid (ABA) method developed for tropical trees (25, 26). Three samples had been previously processed to α-cellulose using the Brendel method (27, 28). A replicate sample of ABA treated samples was prepared using the Brendel technique, in order to provide a confirmation of the radiocarbon-bias correction for $\Delta^{14}C$ measurements on α-cellulose extracted using the Brendel method (28). Extracted wood and cellulose samples were combusted and the purified carbon dioxide reduced to an iron carbide powder over hot zinc for $\Delta^{14}C$ measurement by tandem accelerator mass spectrometer at the University of Arizona AMS Facility (29, 30).

1. Haber WA (2000) in *Monteverde: Ecology and Conservation of a Tropical Cloud Forest*, eds Nadkarni NM, Wheelwright NT (Oxford University Press, Oxford, United Kingdom), pp 39–70.
2. Brown AD and Kappelle M (2001) in *Neotropical Cloud Forests* (Translated from Spanish), eds Kappelle M, Brown AD (Instituto Nacional de la Biodiversidad, Costa Rica), pp 25–40.
3. Bruijnzeel LA (2001) Hydrology of tropical montane cloud forests: A reassessment. *Land Use and Water Resources Research* 1:1–18.
4. Clark KL, Lawton RO, and Butler PR (2000) in *Monteverde: Ecology and Conservation of a Tropical Cloud Forest*, eds Nadkarni NM, Wheelwright NT (Oxford University Press, Oxford, UK), pp 15–38.
5. Treydte K et al. (2006) The twentieth century was the wettest period in northern Pakistan over the past millennium. *Nature* 440:1179–1182.
6. Evans MN and Schrag DP (2004) A stable isotope-based approach to tropical dendroclimatology. *Geochim Cosmochim Acta* 68:3295–3305.
7. Anchukaitis KJ, Evans MN, Wheelwright NT, and Schrag DP (2008) Stable isotope chronology and climate signal in neotropical montane cloud forest trees. *J Geophys Res* 113:G03030.
8. Rozanski K, Araguas-Araguas L, and Gonfiantini R (1993) *Isotopic Patterns in Modern Global Precipitation*, American Geophysical Union Geophysical Monograph ed Swart PK Vol. 78, pp 1–36.
9. Gat JR (1996) Oxygen and hydrogen isotopes in the hydrologic cycle. *Ann Rev Earth Planet Sci* 24:225–262.
10. Lachniet MS and Patterson WP (2002) Stable isotope values of Costa Rican surface waters. *Journal of Hydrology* 260:135–150.
11. Rhodes AL, Guswa AJ, and Newell SE (2006) Seasonal variation in the stable isotopic composition of precipitation in the tropical montane forests of Monteverde, Costa Rica. *Water Resour Res* 42:W11402.
12. Guswa AJ, Rhodes AL, and Newell SE (2007) Importance of orographic precipitation to the water resources of Monteverde, Costa Rica. *Advances in Water Resources* 30:2098–2112.
13. Feild TS and Dawson TE (1998) Water sources used by *Didymopanax pittieri* at different life stages in a tropical cloud forest. *Ecology* 79:1448–1452.
14. Ingraham N and Matthews R (1990) A stable isotopic study of fog—The Point Reyes Peninsula, California, USA. *Chemical Geology* 80:281–290.
15. Fischer DT and Still CJ (2007) Evaluating patterns of fog water deposition and isotopic composition on the California Channel Islands. *Water Resour Res* 43:W04420.
16. Scholl MA, Giambelluca TW, Gingerich SB, Nullet MA, and Loope LL (2007) Cloud water in windward and leeward mountain forests: The stable isotope signature of orographic cloud water. *Water Resour Res* 43:W12411.
17. Pounds JA, Fogden M, and Campbell JH (1999) Biological response to climate change on a tropical mountain. *Nature* 398:611–615.
18. Barbour MM, Roden JS, Farquhar GD, and Ehleringer JR (2004) Expressing leaf water and cellulose oxygen isotope ratios as enrichment above source water reveals evidence of a Peclet effect. *Oecologia* 138:426–435.
19. Evans MN (2007) Toward forward modeling for paleoclimatic proxy signal calibration: a case study with oxygen isotopic composition of tropical woods. *Geochem Geophys Geosyst* 8:Q07008.
20. Linacre E (1964) A note on a feature of leaf and air temperatures. *Agricultural Meteorology* 1:66–72.
21. Gonfiantini R, Roche MA, Olivy JC, Fontes JC, and Zuppi GM (2001) The altitude effect on the isotopic composition of tropical rains. *Chemical Geology* 181:147–167.

22. Kalnay E et al. (1996) The NCEP/NCAR 40-year reanalysis project. *B Am Meteorol Soc* 77:437–471.
23. Kanamitsu M et al. (2002) NCEP-DOE AMIP-II Reanalysis (R-2). *B Am Meteorol Soc* 83:1631–1643.
24. Hua Q, Barbetti M, Worbes M, Head J, and Levchenko VA (1999) Review of radiocarbon data from atmospheric and tree ring samples for the period 1945–1997 AD. *IAWA Journal* 20:261–283.
25. Poussart PF and Schrag DP (2005) Seasonally resolved stable isotope chronologies from northern Thailand deciduous trees. *Earth and Planetary Science Letters* 235:752–765.
26. Westbrook JA, Guilderson TP, and Colinvaux PA (2006) Annual growth rings in a sample of *Hymenaea courbaril*. *IAWA Journal* 27:193–197.
27. Brendel O, Iannetta PPM, and Stewart D (2000) A rapid and simple method to isolate pure α-cellulose. *Phytochemical Analysis* 11:7–10.
28. Anchukaitis KJ et al. (2008) Consequences of a rapid cellulose extraction technique for oxygen isotope and radiocarbon analyses. *Anal Chem* 80:2035–2041.
29. Donahue DJ, Jull AJT, and Toolin LJ (1990) Radiocarbon measurements at the University of Arizona AMS facility. *Nuclear Instruments and Methods B* 52:224–228.
30. Burr GS et al. (2007) Error analysis at the NSF-Arizona AMS facility. *Nuclear Instruments and Methods in Physics Research Section B* 259:149–153.
31. Reimer P, Brown T, and Reimer R (2004) Reporting and calibration of post-bomb 14 C data. *Radiocarbon* 46:1299–1304.
32. Hua Q and Barbetti M (2004) Review of tropospheric bomb ^{14}C data for carbon cycle modeling and age calibration purposes. *Radiocarbon* 46:1273–1298.
33. Bronk Ramsey C (1995) Radiocarbon calibration and analysis of stratigraphy: The OxCal program. *Radiocarbon* 37:425–430.
34. Bronk Ramsey C, van der Plicht J, and Weninger B (2001) "Wiggle matching" radiocarbon dates. *Radiocarbon* 43:381–389.

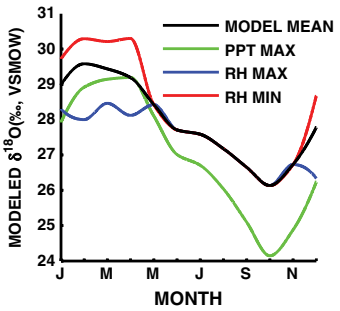

Fig. S1. Process model sensitivity experiments. Model simulations demonstrate that anomalies in the annual $\delta^{18}O$ cycle are generated by higher than normal wet season rainfall (experiment with an imposed maximum observed wet season rainfall, green line) or dry season relative humidity (experiment with an imposed maximum or minimum observed relative humidity, blue and red lines, respectively). Note that the model predicts that wet season rainfall anomalies carry over to the following dry season and influence the annual cycle amplitude in this manner, whereas anomalies associated with changes in relative humidity are confined to the experimentally induced season itself.

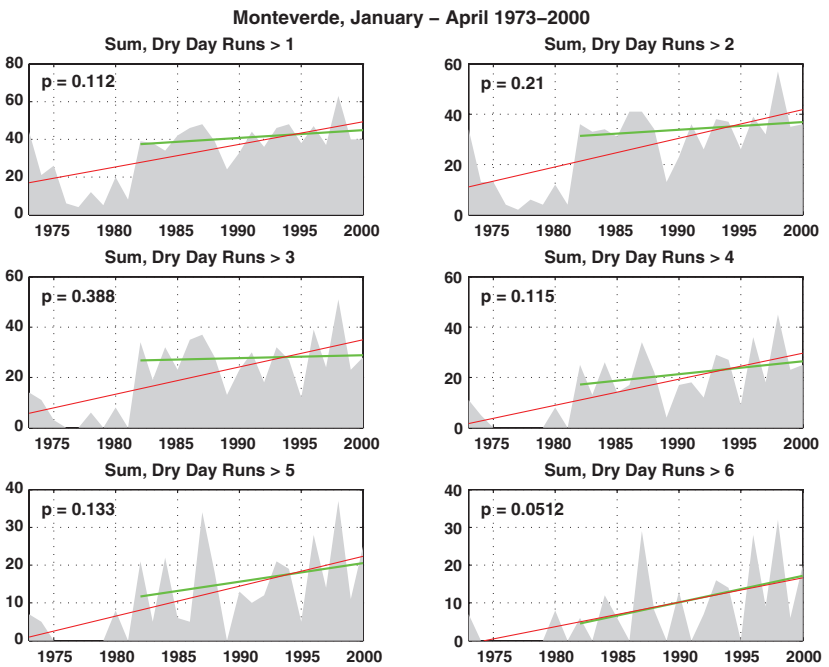

Fig. S2. The sum of dry days during the dry season in consecutive blocks longer than a given threshold, indicated above each plot. Least-squares trends for 1973–2000 are shown by the red lines, and for 1983–2000 by the green lines. The magnitude and significance (*p*-values are shown for the later period) of the trend is a function of the time period and the chosen threshold.

Table S1. Radiocarbon summary

Sample	AA74375	AA74376	AA74377	AA776775	AA74381	AA74379	AA74378
Core	MV12	MV12	MV12	MV15	MV15	MV15	MV15
Depth (mm)	167	230	242	19.5	57	69	121
Initial data							
Fraction modern carbon (F14C)	1.5111	1.0842	0.992	1.126	0.9859	0.9882	0.9833
Measurement precision	0.0078	0.0088	0.004	0.0048	0.0069	0.006	0.004
2σ calibrated date (A.D.)	1969–1972	1955–1957	1951–1956	1957–1961	1526 (2.7) 1556 1632 (77.1) 1894 1905 (15.6) 1954	1646 (21.0) 1710 1716 (57.5) 1890 1909 (16.9) 1954	1669 (41.1) 1780 1798 (39.0) 1893 1906 (15.2) 1944
Bayesian calibration							
Posteriori 2σ range A.D.					1938–1939	1931–1932	1908–1909
% Agreement					120.8	114.9	67.5
Model agreement (threshold)							96.8 (35.4)

Radiocarbon analysis from MV12 and MV15. Calibrated dates are shown with the percentage of the probability density function associated with each range of years. Post-bomb calibrated dates include any additional uncertainty associated with using different atmospheric $\Delta^{14}C$ curves (31, 32). Bayesian analysis for development of a posteriori probability functions was performed using OxCal, applying the known temporal (stratigraphic) order of the dates and the estimated annual increment based on the $\delta^{18}O$ chronology (33, 34). Agreement scores for the Bayesian calibration are uniformly above 60% for the individual dates and exceeds the lower minimum threshold (~35%) for the model as a whole (33). F14C values have been corrected for those samples prepared with the Brendel method (28) and discussed here in the supporting text. Uncertainty due to this correction is substantially smaller than radiocarbon measurement precision in these cases.